Energy Equip. Sys./ Vol. 12/No. 4/December 2024/ 399-421

ENERGY EQUIPSYS

Energy Equipment and Systems

www.energyequipsys.com

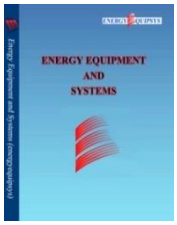

Numerical study of thermal management and performance enhancement of finned solar cells by phase change materials

Manuscript Type
Research Paper

Authors

Hesam Jiryaei Sharahi[a]
Amir Masoud Roshan[a]
Mehdi Moghimi[a*]

[a] School of Mechanical Engineering, Iran University of Science and Technology, Tehran, Iran.

Article history:

Received : 16 March 2024
Revised : 24 August 2024
Accepted : 9 September 2024

ABSTRACT

The unfavorable heat generation in the photovoltaic (PV) panels results in an increased average temperature of PV, followed by decreased electrical performance of the entire system. One can reduce the average temperature of the photovoltaic panel using a phase change material (PCM) at its back which improves the electrical efficiency of the photovoltaic panel. Nonetheless, the low thermal conductivity of the phase change material leads to its poor cooling efficiency. The application of fins can enhance heat transfer through PCM. This investigation conducts a numerical estimation of the geometrical improvement of fins in a phase change material integrated the PV system featuring interior fins. The contribution of geometrical characteristics, such as type, fin length, shape, and also disposition angle, to the efficiency of the PCM amalgamated the PV module has been investigated. In addition, when the fin length is increased from 0 to 20mm, the efficiency and operating temperature of the photovoltaic panel improved by 3.5% and 2.7%, respectively. To investigate the impact of shape of the fin on its cooling performance, five different fin shapes have been considered. The results show that triple-branched fins exhibited 1.2% and 1.5% augmentation in the mean working temperature of the PV module and performance of the system, respectively, when compared to the traditional rectangular fins. Moreover, comparative results indicate that compared to the conventional rectangular PCM encapsulation, in the case of employing non-rectangular PCM encapsulations with higher top-to-bottom ratio higher cooling performance and melting rate of PCM is achieved. So with this change in PCM encapsulations, the temperature of the system can be reduced by 2.28 °C.

Keywords: Phase Change Material, Solar Cell, Thermal Management, Fins, Heat Transfer.

1. Introduction

The last century has witnessed a boom in research into improving the efficiency of solar panels. In a photovoltaic cell (PV cell), just 15-20% of the received solar energy is used to generate electricity, and the remnant of this energy is wasted in the form of generated heat [1]. The consistency of the semiconductor used, the strength of the solar radiation, and the working temperature of the PV systems all have a role in the electrical productivity of the

[*] Corresponding author: Mehdi Moghimi
School of Mechanical Engineering, Iran University of Science and Technology, Tehran, Iran.
Email: moghimi@iust.ac.ir

PV systems. The electrical efficiency of solar systems is affected differently by improving the average temperature of PV. An increase of 1°C in its average temperature results in a decrease of 0.5% in its electrical efficiency [2]. As a result, extraction of excess heat from the PV cells is necessary to improve the efficiency of solar panels. It is possible to boost electricity efficiency by adopting photovoltaic thermal systems (PVT) by lowering PV's temperature. The three most frequently used types of PVT systems are air-cooled, phase change material (PCM) cooled, and water-cooled systems [3]. Due to the high freezing temperature of water, the water-cooled PVT modules are not functional in cold regions. Moreover, due to the low specific heat of air, the air-cooled PVT modules are not effective. To achieve its melting point, the solid PCM in a PVT-PCM module absorbs heat from the solar panel, and, as a result, its temperature rises. As a result, PCM-cooled systems can store energy and operate as the energy supply in the absence of sunlight at night and also passively increase the system's efficiency. The main technical issue of the PVPCM systems is that the performance of PCM is considerably restricted by the poor thermal conductivity of PCM. To improve the undesirable low heat conductivity of PCM different modifications have been suggested, such as the insertion of metal foam [4–7], the addition of nanoparticles into the PCM [8–12], and the installation of fins [13–15].

Many researchers have studied the impact of the insertion of metal and other conductive foams into the PCM. The irregular motion of the fluid through the porous metal foam leads to the augmentation in the thermal conductivity of PCM [4]. Owing to the easy fabrication, low cost, and high specific surface area, insertion of conductive porous foams has become one of the most effective approaches to increase the thermal conductivity of PCMs [16], [17]. The porous media are mainly characterized by porosity and pore diameter. In their comparative investigation, Hussain et al. [18] studied the pore diameter and porosity of Ni foam inserted into paraffin. Their findings [18] showed that, with a porosity of 0.97, Ni/paraffin showed a 500% increase in thermal conductance compared to pure phase change material. Badenhorst [19] investigated the reinforcement of the thermal conductivity of PCMs by employing various carbon-based systems, like graphite foams, graphite fibers, amorphous carbon, and graphite nanoplates. The results indicated that by adding matrix materials such as graphite foams into PCM, a 10000% improvement factor is achieved. The most concerning issue of this method is the reduction of available space in PCM containers. As a result, metal foams containing gradient porosity have been proposed to expand the volume of PCM. Scalar evaluations conducted by Ami Ahmadi et al. [4] led to the discovering the ideal metal foam arrangement. Compared to a porous foam containing a uniform porosity of 0.795, the findings showed that embedding a conductive porous foam with greater porosity from the bottom to the top may increase PCM charging duration by up to 3.35 percent.

The inclusion of conductive nanomaterials in the phase change material may also speed up the heat transfer. Using random movements of nanoparticles, known as Brownian motion, the thermal conductivity of PCM is improved [20]. To study the impact of nanoparticles on the melting process of PCM and the overall efficiency of the PV module, Abdelrahman et al. [10] carried out a series of experimental investigations on the impact of employing PCM with mixed Al2O3 nanoparticles with varying volume fractions from 0.11% to 0.77%. The results demonstrated that in a PVPCM system with nanoparticles, a 52.3% drop in the temperature of PV module is obtained. Moreover, research have been conducted to examine the thermal conductivity of PCM mixed with hybrid nanoparticles [21], [22]. Pasupathi et al. [22] experimented with the impact of hybrid nanoparticles on the thermos-physical characteristics of PCM. In this study, the authors added a combination of SiO2 and CeO2 to the paraffin-based PCM. The results indicated that employing hybrid nanoparticles elevates the relative thermal conductivity up to 165.56%.

Installation of fixed structures such as fins is one of the most effective innovative approaches to enhance the cooling performance of PCM. The use of metal fins in the PCM container has been proved by several studies to improve thermal conductivity using the PCM container by raising the conductivity area. Biwole et al.

[13] executed a numerical investigation on the influence of PCM and the induction of fins into the PCM vessel on the cooling efficiency of PCM. Insertion of metal fins into the PCM vessel reduces the temperature of the PV cell by 56.9% relative to a PV module devoid of any cooling approaches. One of the most influential parameters in the design of metal fins is the geometry of fins, which can considerably affect the heat transfer by the PCM. To investigate the influence of geometrical parameters, such as fin spacing, fin thickness, and fin length, Khanna et al. [23] have conducted a comparative study and obtained an optimum fin design. Moreover, to study the other geometrical properties, Benlekkam et al. [24] carried out numerical research on the impact of fin orientation and its tilt angle on the performance of Al fins. The comparative results represented that employing metal fins with a tilt angle of 25° preserved the electrical efficiency of PV cells at 14%, which indicates an almost 2% enhancement compared to the horizontal fins.

It must be noted that the operating conditions can effectively influence the efficiency of the PVPCM module. The contribution of working climate and fin spacing to the efficiency of PVPCM modules equipped with metal fins was numerically investigated by Khanna et al. [25]. Khanna et al. [25] demonstrated that the improvement in the performance of fins for different fin spacing is significantly dependent on the operating climate. For less altering climates, the enhancement of output electrical efficiency of PV cell is 11.6%, 11.6%, 11.3%, 10.8%, and 9.7%, respectively, for fin spacing of 1/5m, 1/4m, 1/3m, 1/2m, and 1m. On the other hand, for more altering operating conditions, the values of electrical efficiency for the same fin spacing drop to 8.4%, 8.4%, 8.1%, 7.6%, and 6.6%, respectively. Furthermore, the results showed a considerable enhancement in the performance of finned PCM in a clear sky.

Recently, other innovative approaches have been proposed to augment the efficiency of PV systems integrated with phase change material. Recent advances in the PCM-integrated PV systems indicate that the disposition angle and shape of PCM containers can drastically improve the overall efficiency of PVPCM systems. A numerical study conducted by Khanna et al. [26] on the effect of tilt angle on the PV/PCM system was carried out to examine this angle deeper. The results of this study demonstrated that an increment of the inclination angle from 0° to 90° results in the decrement of the temperature of PV panel from 43.4°C to 34.5°C, respectively. Thermal conductivity is the predominant mode of heat transfer in solid PCMs. Convective heat transfer, on the other hand, increases when the PCM dissolves. Recent studies demonstrate that in a conventional rectangular PCM container, convective currents are suppressed. Therefore, the application of non-rectangular containers has been suggested. In order to achieve an optimal design for the encapsulation of phase change material, Ahmad et al. [27] studied the contribution of the container shape to the cooling efficiency of the phase change material. According to their results, a trapezoid-shaped container demonstrates an improved cooling efficiency compared to rectangular-shaped ones. Also, Akshayveer et al. [3] proposed an optimized design for the PCM encapsulation in which a 17% enhancement in the melting rate of the PCM is observed. Moreover, Akshayveer et al. [3] demonstrated that by employing the proposed PCM encapsulation, the temperature of PV cells drops up to 11.5%, consequently the efficiency of PV extents to 12%. Other passive cooling approaches, including metal foams and fins mixture [28] and various phase change materials containing various melting temperatures [29], have recently been suggested to improve the electrical performance of PV systems.

According to the literature review, there is a limited investigation on the effect of fin characteristics on system performance. As a result, to reach an optimal fin design, the present paper carried out numerical research to study the contribution of geometrical specifications of fins to the electrical performance and heat transfer improvement of a PV system. To obtain the most efficient fin design, the following fin characteristics have been studied individually: fin length, vertical position, fin type, fin shape, and fin material. Moreover, many researchers have established that the geometrical properties of PCM encapsulation can shorten the phase change process of PCM effectively. It is evident that the conventional rectangular PCM encapsulation design does not aid in natural convection, and there is limited research on PVPCM systems with asymmetrical PCM

enclosures. In the current study, we have presented research on an innovative PCM encapsulation design that promotes natural convection, leading to improved melting rates and heat transfer efficiency. As a result, the effect of PCM entrapment's tilt angle and layout on thermal conductivity and PCM melting has been examined during the present work. The main objective of this study is the parametric analysis of geometrical characteristics of fins and novel PCM encapsulation designs.

Nomenclature

Symbols

α	Thermal diffusivity ($m^2.s^{-1}$)
B_0	Melt function
B_1	Smoothed melt function
C_p	Specific heat ($J.kg^{-1}K^{-1}$)
D	Smoothed delta Dirac function
F_A	Added force due to phase change ($N.m^{-3}$)
F_b	Buoyancy force ($N.m^{-3}$)
g	Gravitational acceleration ($m.s^{-2}$)
H	PCM container height (m)
h_e	Outdoor convective heat transfer coefficient ($W.m^{-2}K^{-1}$)
h_i	Indoor convective heat transfer coefficient ($W.m^{-2}K^{-1}$)
k	Thermal conductivity ($W.m^{-1}K^{-1}$)
L_F	Latent heat of fusion ($J.kg^{-1}$)
L	PCM container width (m)
m	Mass (kg)
P	Pressure (Pa)
T	Temperature (K)
T_m	Melting point (K)
u	Velocity ($m.s^{-1}$)
ΔT	Half range of melt temperatures (K)
Δx	Maximum length of grids (m)

Greek symbols

β	Thermal expansion coefficient (K^{-1})
ε	Computational constant
ρ	Density ($kg.m^{-3}$)
μ	Dynamic viscosity (Pa.s)
ν	Kinematic viscosity ($m^2.s^{-1}$)

Subscripts

liquid	Liquid
PCM	Phase change material
solid	Solid

Abbreviation

PCM	Phase change material
PV	Photovoltaic system
PVT	Photovoltaic thermal system

2. Problem description

The physical model employed in the current study is portrayed in Fig. 1. The computational model consists of an aluminum container filled with PCM. Aluminum fins are put inside the PCM container to improve thermal conductivity. The temperature of PCM increases to its melting point due to the heat produced in the PV cell. The dimensions of the applied model in the current numerical simulation are presented in Table 1. To imitate the solar irradiation, an inward heat flux with the value of 1000 W/m2 is applied on the left outer wall.

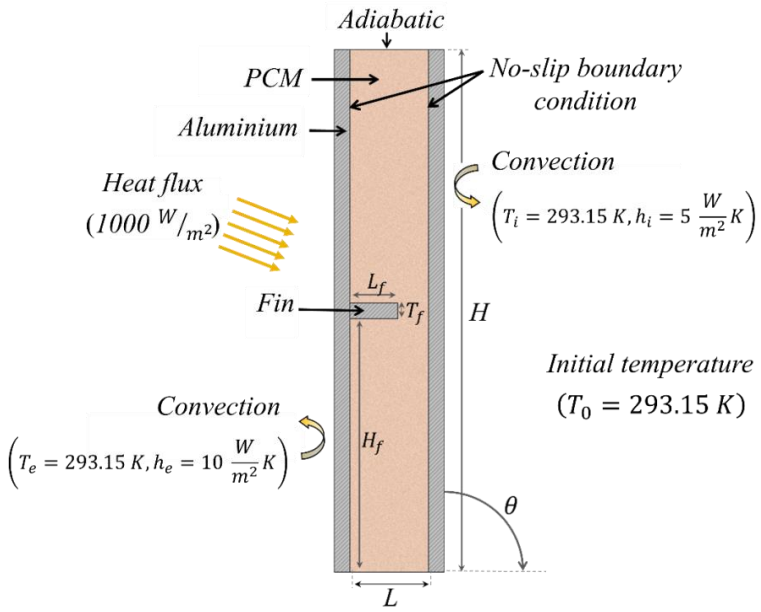

Fig. 1. Schematic of the computational model

Table 1. Geometry properties

	Thickness	Length
Aluminum walls	4 mm	132 mm
PCM container	20 mm	132 mm
Fin	0-4 mm	0-20 mm

To investigate the influence of the geometrical properties of the fin on its performance, the length of fins is inspected in ranges of 0-20mm. Additionally, in order to achieve the most effective fin shape, in the present study, fins with innovative shapes are studied (Fig. 2).

Besides, the present paper deals with the impacts of the fins' vertical position on the PCM's phase alteration procedure. To investigate the effect of vertical position, five cases with a single metal fin located on the left wall at a distance of 21, 44, 66, 88, and 111mm from the bottom are studied (Fig. 3). Moreover, the geometrical properties of PCM encapsulation, such as inclination angle (θ) and the encapsulation design (rectangular or non-rectangular PCM containers), are investigated. The impact of module disposition angle on the improved heat transfer within PCM was studied considering the angles of 0°, 22.5°, 45°, 67.5°, and 90°.

In the present study, Paraffin RT25 is adopted as the phase change material. Paraffin RT25 has a melting temperature of 25 °C, which aligns with the reference temperature of the photovoltaic panel. This compatibility ensures inefficient heat absorption during the phase change process. The thermophysical properties of paraffin RT25 and aluminum are given in Table 2.

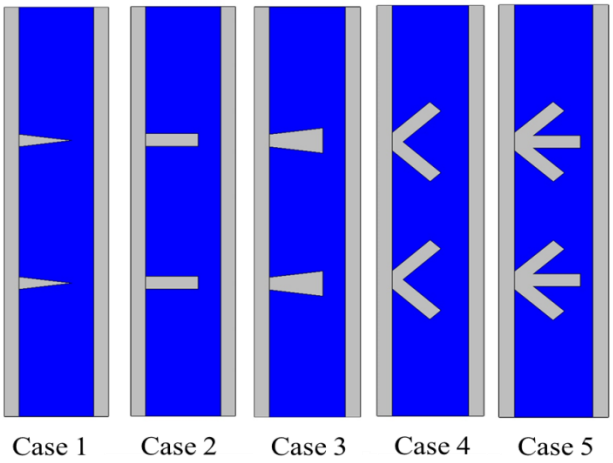

Fig. 2. Schematic of the fin types

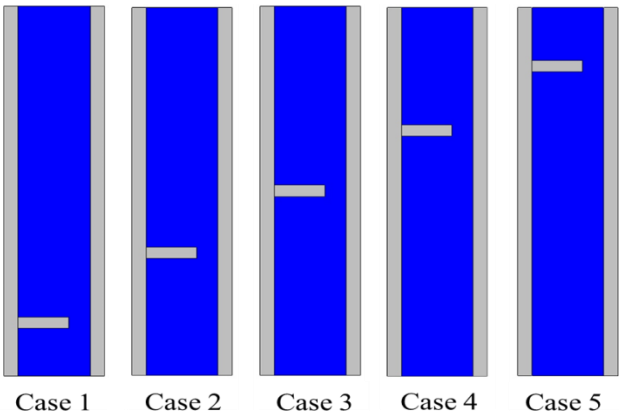

Fig. 3. Schematic of the vertical position of a single fin

Table 2. Thermophysical properties of materials [13], [30]

	Units	RT25	Aluminum
Density (ρ)	kg/m^3	785 (S) 749 (L)	2675
Specific heat (C_p)	$J/kg.K$	1800 (S) 2400 (L)	903
Thermal conductivity (k)	$W/m.K$	0.19 (S) 0.18 (L)	211
Heat of fusion (L_F)	J/kg	232000	-
Melt temperature (T_m)	℃	26.6	-
Dynamic viscosity (μ)	m^2/s	1.7986×10^{-3}	-
Thermal expansion coefficient (β)	K^{-1}	0.001	-

2.1. Boundary and initial conditions

In the current research, the following boundary and initial conditions are considered:

- To imitate the solar radiation, a heat flux equal to 1000 W/m^2 is applied on the left outer wall. Additionally, a convective heat transfer on the left wall is applied. (T_e =293.15K, h_e =10 W/m^{2}K).
- On the right outer wall, convective heat flux is applied. The ambient temperature (T_i) is set to 293.15 K. Moreover, the convective heat transfer coefficient is h_i = 5 W/m^{2}K.
- A no-slip boundary condition is set on the inner walls of the PCM container.
- All the remaining outer walls are set to be adiabatic.
- The initial temperature of the system is 293.15 K.

2.2. Governing equations

To investigate the electrical efficiency of PV cell, it is essential to study the heat transfer in PV cell, aluminum, and PCM domains. To replicate the heat transfer in the PV system and aluminum domains, the governing equation of energy conservation is defined as follows [13]:

$$\rho C_p \frac{\partial T}{\partial t} = -k\frac{\partial T}{\partial x} + h_e\left(T_e - T\right) + \alpha E\left(t\right) \quad (1)$$

In the above equation, the ρ, Cp, k, and he denote the density, specific heat, thermal conductivity, and outdoor convective heat transfer, respectively. α and E(t) represent the absorption coefficient of aluminum and solar irradiation. The terms on the right side of Eq. (1) respectively signify the conductive heat transfer, convection between the outdoor air, and PV cell and absorbed solar radiation. In this paper, the radiative heat loss from PV cell to the sky is neglected. Also, to analyze the phase change process and heat transfer in the PCM area, the equations of conservation of energy, mass, and momentum presented below have been utilized [13].

$$\frac{\partial \rho_{PCM}}{\partial t} + \nabla.\left(\rho_{PCM}\vec{u}_{PCM}\right) = 0 \quad (2)$$

$$\frac{\partial \rho_{PCM}}{\partial t} + \nabla.\left(\rho_{PCM}\vec{u}_{PCM}\right) = 0 \quad (3)$$

$$\rho_{PCM}\frac{\partial \vec{u}_{PCM}}{\partial t} + \rho_{PCM}\left(\vec{u}_{PCM}.\nabla\right)\vec{u}_{PCM} - \mu.\nabla^2\vec{u}_{PCM} = -\nabla P + \vec{F}_B + \vec{F}_a \quad (4)$$

where μ, $\vec{u}$, and P are the viscosity of PCM, velocity vector, and pressure. In Eq.3, $\vec{F}_B$ denotes the buoyancy force evaluated by Boussinesq approximation (Eq.5) [13].

$$\vec{F}_B = -\rho_{liquid}\left(1-\beta\left(T-T_m\right)\right)\vec{g} \quad (5)$$

In the above equation, ρ_{liquid} and $\vec{g}$ represent the density of molten PCM and gravitational acceleration. Also, β denotes the thermal expansion coefficient. Accounting for the impact of latent heat, $\vec{F}_a$ is considered in the momentum conservation equation, which describes the pressure drop through the porous medium (mushy zone) [13].

$$\vec{F}_a = -A(T).\vec{u} \quad (6)$$

$A(T)$is a temperature-dependent expression, which is calculated in the form of Carman-Kozeny correlation [23]:

$$A(T) = \frac{C\left(1-B_1(T)\right)^2}{\left(B_1(T)^3+\varepsilon\right)} \quad (7)$$

C and ε denote the mushy zone constant and a small computational constant equal to

0.001[4]. Mushy zone constant is significantly affected by the morphology of the medium and typically takes the values from 10^5 to 10^9 [3]. In the current work, the value of C is 10^5, moreover, in Eq. $B_1(T)$, it is the mass fraction of PCM. One of the most eminent methods in calculating the liquid fraction and modeling the charging process of PCM is the enthalpy porosity approach. The enthalpy porosity approach describes the phase change material as a porous medium referred to as a mushy zone, which consists of liquid phase change material dispersed into solid PCM [4]. Thus, the porosity of the mushy zone is represented by the value of liquid mass fraction B_0, which takes the values of 0, $0<B_0<1$ and 1, respectively, in the solid phase, mushy zone, and molten phase. To calculate the value of B_0, the following correlation is employed [13]:

$$B_0 = \begin{cases} 0 & T < (T_m - \Delta T) \\ \dfrac{T - T_m + \Delta T}{2\Delta T} & (T_m - \Delta T) < T < (T_m + \Delta T) \\ 1 & T > (T_m - \Delta T) \end{cases} \quad (8)$$

where T, T_m, and ΔT denote temperature, melting temperature of PCM, and the half range of melt temperature. To enhance the convergence, the liquid fraction is estimated by $B_1(T)$, a second-order continuous differentiable function. $B_1(T)$ is a six-degree polynomial function given in Eq.9. To derive the coefficients of $B_1(T)$, the following conditions are employed [23].

$$B_1(T) = \sum_{i=0}^{6} a_i T^i \quad (9)$$

$$\begin{aligned} &B_1(T_m - \Delta T) = 0 \,, B_1'(T_m - \Delta T) = 0 \,, \\ &B_1''(T_m - \Delta T) = 0 \,, B_1(T_m) = 0.5 \,, \\ &B_1(T_m + \Delta T) = 1 \,, B_1'(T_m + \Delta T) = 0 \,, B_1'(T_m + \Delta T) = 0 \end{aligned} \quad (10)$$

2.2.1. Thermophysical properties of PCM

The melting and solidification process leads to significant alterations in the thermophysical properties of PCM. Therefore, to capture the changes mentioned above, and enhance the convergence, it is essential to propose appropriate functions. In this paper, the following functions for thermal conductivity, density, and specific heat of PCM are applied [23].

$$\rho(T) = \rho_{solid} + (\rho_{liquid} - \rho_{solid}).B_1(T) \quad (11)$$

$$k(T) = k_{solid} + (k_{liquid} - k_{solid}).B_1(T) \quad (12)$$

$$C_p(T) = C_{psolid} + (C_{pliquid} - C_{psolid}).B_1(T) + L_F.D(T) \quad (13)$$

where subscripts $solid$ and $liquid$ denote the thermophysical property of solid and melted PCM, respectively. Moreover, the $D(T)$ in Eq. 12 is given by the following correlation [23]:

$$D(T) = \frac{e^{-(T-T_m)^2/(\Delta T/4)^2}}{\sqrt{\pi(\Delta T/4)^2}} \quad (14)$$

2.2.2. Efficiency of PV cell

The electrical efficiency of a PV system significantly depends on the mean temperature of the photovoltaic cells. Therefore, to account for the influence of the mean temperature of the PV system, Evans and Florschutez introduced the following equation [31]:

$$\eta_{PV} = \eta_{ref}\left[1 - \beta_{ref}\left(T - T_{ref}\right)\right] \quad (15)$$

where η_{ref} represents the electrical efficiency at the reference temperature ($T_{ref} = 25℃$). Also, β_{ref} is the temperature coefficient of PV cell. In the current study, the values of η_{ref} and β_{ref} are 0.124 and 0.00392, as reported by Evans and Florschutez [31].

3. Numerical simulation

In order to simulate the transient heat transfer, to solve the conservation equations, a two-dimensional CFD simulation has been conducted. In addition, a SIMPLE scheme is used in order to resolve the pressure-velocity coupling. Due to the time-dependent heat transfer, the implicit finite volume method is used. A second-order scheme is used for spatial and temporal discretization. Moreover, the numerical simulations are performed using the CFD software ANSYS-Fluent. The mesh is created by employing a 2D quadrilateral grid as shown in Fig.4b. To ensure the grid independency, three sets of meshes with different mesh sizes of 1mm, 0.5mm, and 0.25mm have been investigated. Figure 4a represents the temperature of the PV system in the first 100 minutes of simulation for different grids. The results indicate an insignificant deviation of 1.02% and 0.45%, demonstrating that grid size 0.5 is accurate enough.

Furthermore, to investigate the sufficient time step, the average PV temperature for two-time steps of 0.5s and 0.25s is studied. Numerical investigations demonstrated 0.204% deviance in results, demonstrating that the time step of 0.5s is sufficiently precise.

3.1. Model validation

The divergence of our calculations with those represented by Biowole et al. [13] was examined in order to validate the results of the present numerical calculations. The model includes an aluminum container that is filled with RT25 acting as the PCM. In order to improve the heat conductivity of the PCM, a pair of horizontal fins is mounted on the left inner wall. Fins are equally spaced, and the widths of fins are 4 mm each. To imitate solar irradiation, a constant heat flux of 1000W/m2 is considered on the left aluminum wall. Moreover, convective heat transfer with the ambient air is considered on the left and right outer walls. The difference between the numerical results of Biowole et al. [13] and the present study is illustrated in Fig. 5, in which the transient operating temperature of the panel is reported. The maximum deviance of 0.507% demonstrates that the current model is in sufficient agreement with the numerical study of Biowole et al. [13].

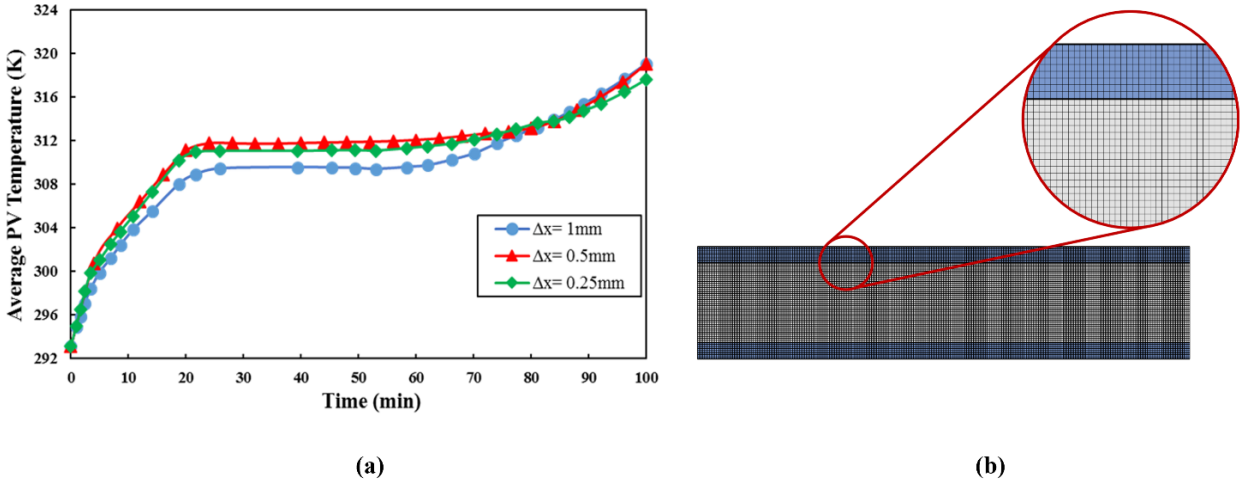

Fig. 4. (a) Average PV temperature of three grids after 100 minutes and (b) The structured grid of the PVPCM panel

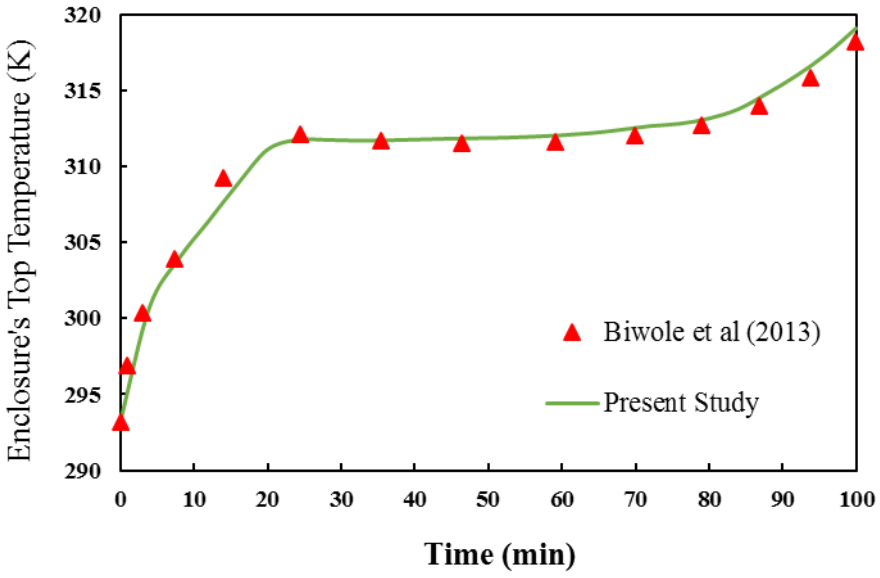

Fig. 5. A comparison between results reported by Biwole et al. [13] and the results of the present study

4. Results and discussion

As previously stated, the PV-PCM cooling performance was augmented by taking into account the impacts of fins' geometrical features including type and length on the behavior of fins. Furthermore, the effects of the inclination angle and encapsulation design of the PV system were also evaluated.

4.1. Effect of fin length

With the pursuit of investigating the influence of the length of fins on the electrical efficiency of the panel and the thermal conductivity of PCM, seven cases of PCM integrated PV systems with three inner aluminum fins are considered. In all cases the width of fins is 4mm each; however, the length of fins varies from 0 to 20mm.

Figures 6 and 7 illustrate the mean temperature and electrical performance of the PVPCM system after solar radiation exposure of 100 min, for fins with a length of 0-20 mm. It was indicated that the PVPCM heat extraction rate was elevated significantly for fins with larger lengths. As a result, given the improved heat transfer in the phase change material domain, a shorter phase change procedure followed by improved electrical performance will be acquired for longer fins. Furthermore, 2.7% and 3.5% improvement, respectively, in the working temperature and efficiency of the PV module in the PCM integrated PV system with a fin length of 20mm is obtained. At the start of the process, when the PCM has not yet melted, Fig. 7 shows a steep decline for the electrical efficiency of the photovoltaic module. This high slope occurs because the thermal energy from the solar is being absorbed by the PCM as sensible heat. The PV module temperature rises rapidly as it accumulates this sensible heat energy. So, a high slope indicates a significant amount of heat absorption and thus a steep decrease in module efficiency. During the middle phase of the process, when the PCM starts to change phase and undergoes melting, the plot of changes in the electrical efficiency appears almost constant. This phase-changing stage involves the absorption of latent heat energy by the PCM as it changes from a solid to a liquid state. While the PCM is absorbing this latent heat, its temperature remains relatively constant even though it is still receiving heat energy. So, between 30 and 70 minutes, the electrical efficiency changes are almost constant.

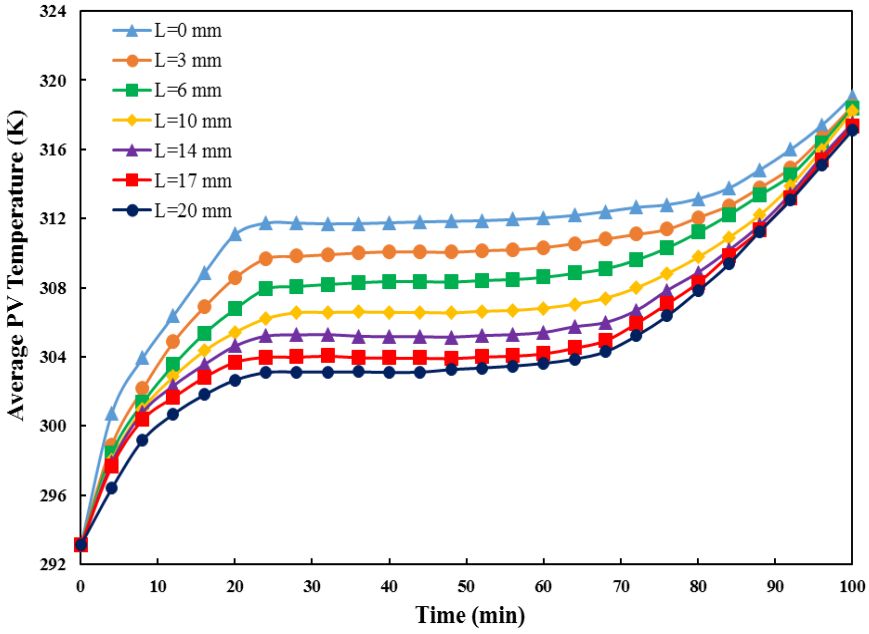

Fig. 6. Mean operating temperature of the photovoltaic module during a simulation of 100 minutes for fin Lengths ranging between 0 and 20mm

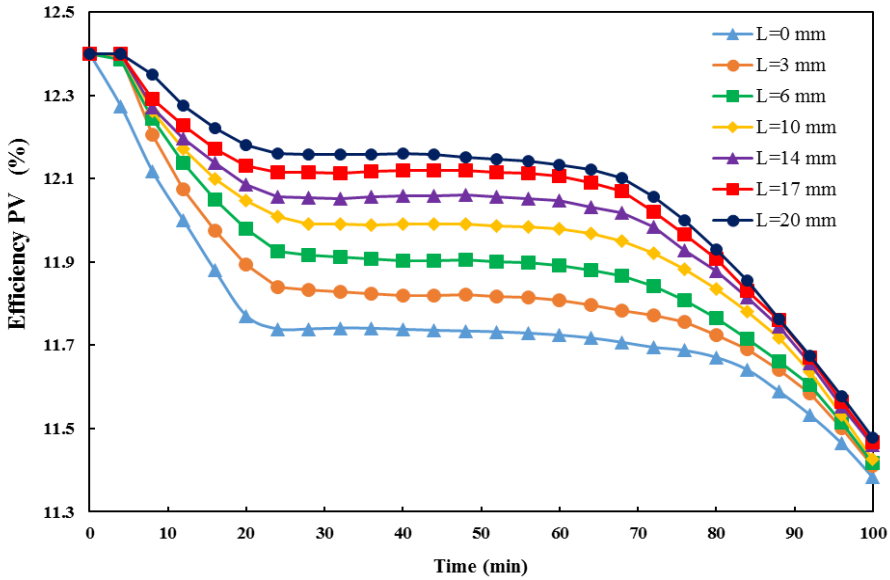

Fig. 7. Electrical efficiency of the photovoltaic module during a simulation of 100 minutes for fin Lengths ranging between 0 to 20mm

Despite the significant influence of metal fins on heat transfer improvement, it must be noted that the application of fins can interrupt the natural flow of melted PCM caused by natural convection. Figure 8 represents the liquid mass fraction of PCM for different fin lengths. Results designate that for longer fins, the aforementioned interruption of the natural flow of molten PCM is more significant. In the initial stages of the process, viscous forces play a significant role due to the thinness of the melting layer, causing the solid-liquid interface to remain parallel to the adjacent wall of the PV panel as these forces counteract fluid flow in this heat transfer mode. As time progresses, the thickness of the melting layer increases and buoyancy forces eventually surpass viscous forces. This transition triggers the onset of natural convection in the melting fluid, leading to the erosion of the solid-liquid interface at the top portion of the melting region. The erosion becomes noticeable by the 60-minute mark, even though natural convection starts influencing the process early on. The emergence of buoyant forces stimulates a circulating current in the upper part of the enclosure, resulting in a concave curvature at the top of the melting front, while the melting front in the rest of the cavity remains nearly linear, with its inclination increasing over time.

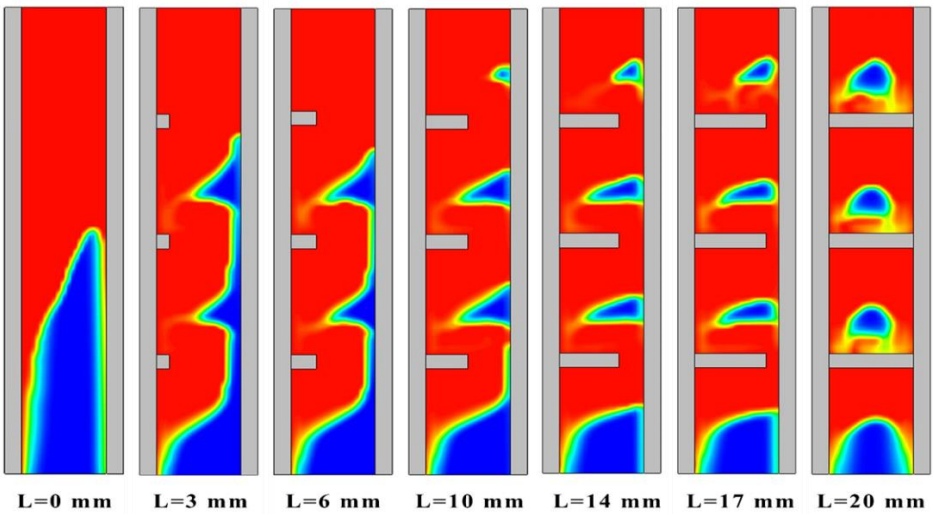

Fig. 8. Liquid mass fraction at Time=60mins for different fin Lengths

4.2. Effect of the vertical position of fins

To investigate the impacts of the fins' vertical position on their cooling behavior, the melting procedure of PCM was studied for PCM-integrated PV systems with a single fin and various vertical locations (Fig. 9). The electrical efficiency and operating PV temperature of the system for various vertical positions (21, 44, 66, 88, and 111mm) are presented in Figs. 10 and 11.

When the PCM melts, natural convection becomes prominent in the liquid part. Natural convection is the process where warmer, less dense material rises while cooler, denser material sinks. This creates a convective flow within the liquid part of the container, aiding heat transfer and mixing. Placing the fin in the lower part of the container has a more pronounced effect on heat transfer. Since conduction dominates heat transfer in the lower parts, adding a fin here helps increase the surface area for heat transfer, facilitating faster melting of the PCM. On the other hand, placing the fin in the upper part might not yield as significant an improvement since natural convection already enhances heat transfer in that region. The fin might disrupt the natural convection currents and potentially hinder the overall melting process by altering the flow patterns. Therefore, strategically placing the fin in the lower part of the container can maximize heat transfer efficiency and accelerate the melting process of the PCM. By changing the vertical position of the fins, the melting time of the PCM can be reduced by up to 12 minutes (Fig. 9). Figure 11 shows that the cooling performance of a single fin at the lower parts is much more significant than higher located fins.

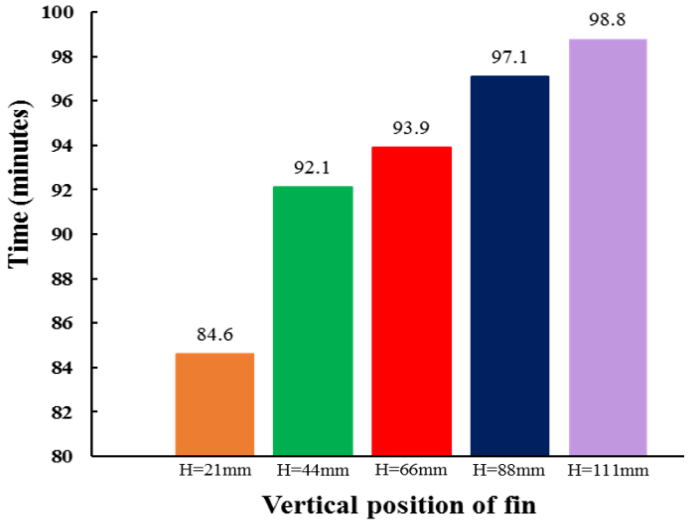

Fig. 9. Melting time of phase change material for various vertical positions of an individual fin

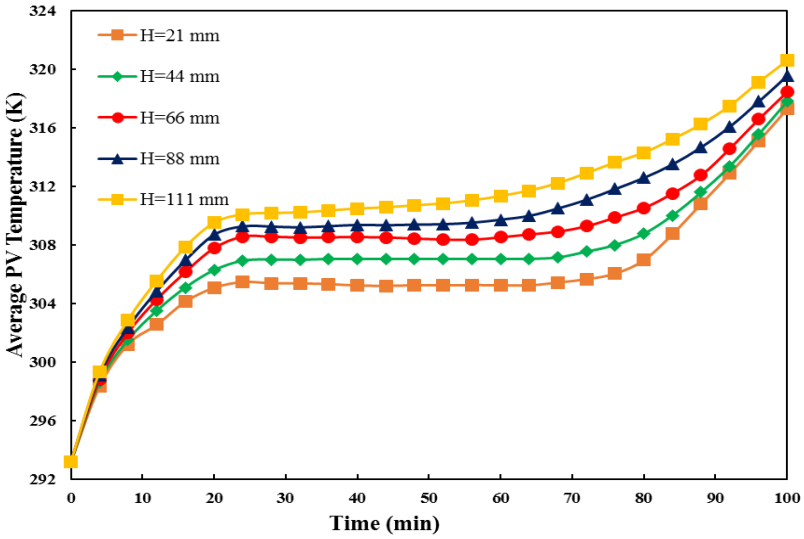

Fig. 10. Mean temperature of the photovoltaic module during a simulation of 100 minutes for various vertical positions of an individual fin

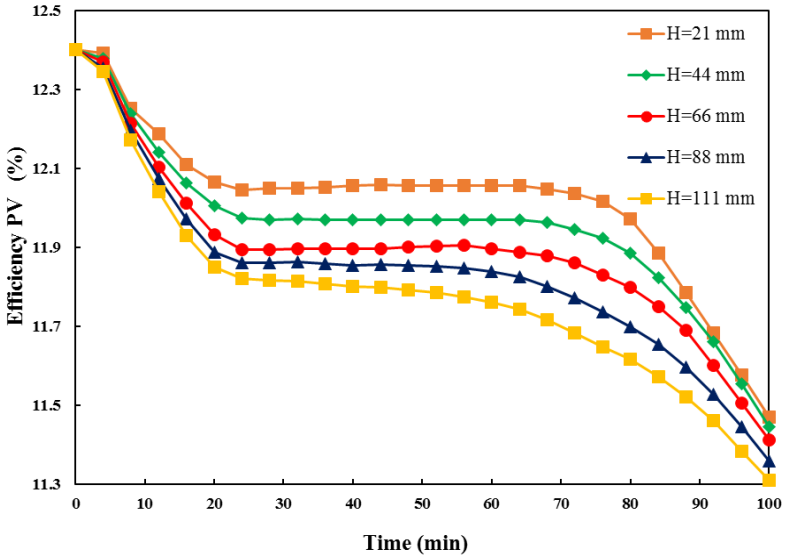

Fig. 11. Electrical efficiency of the photovoltaic module during a simulation of 100 minutes for various vertical positions of an individual fin

4.3. Effect of fin shape

The shape of fins can drastically affect the heat extraction from PV and, eventually, the phase change time of PCM. As the surface area of fins elevates, the heat transfer to the PCM enhances. However, it must be noted that fins with a higher surface area occupy a larger space in the container, which diminishes the PCM mass in the container. Therefore, the shape of the fins must be chosen wisely. With the purpose of finding the optimum fin shape, in the current study, the cooling performance of five fin shapes, needle, rectangular, trapezoid, dual-branch, and triple-branch, is examined (Fig. 2). Figures 12-14 display the melting time, the PV's average temperature, and the PV-PCM system's electrical efficiency for various fin shapes, respectively. According to the findings, the triple-branch fins yielded the least melting time and by changing the shape of the fins from case1 to case5, the melting time of the PCM can be reduced by up to 7 minutes (Fig. 12).

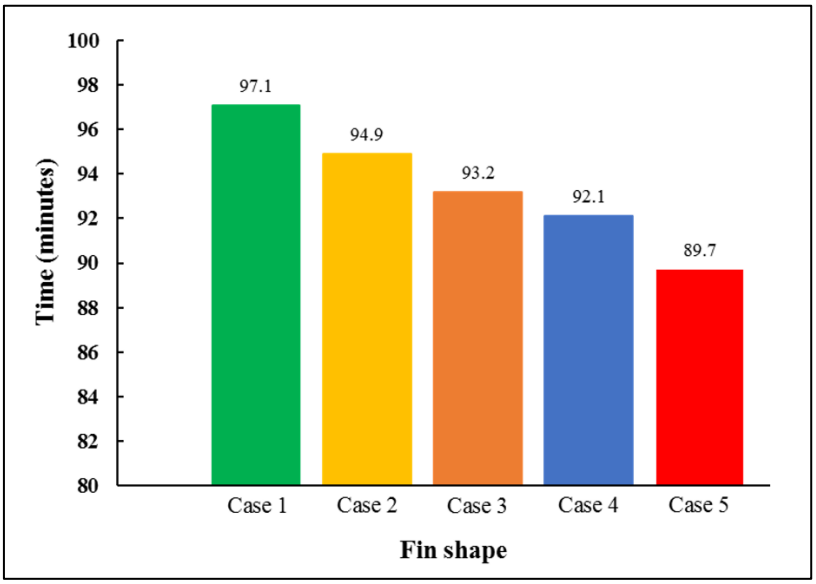

Fig. 12. Melting time of phase change material for a variety of fin shapes

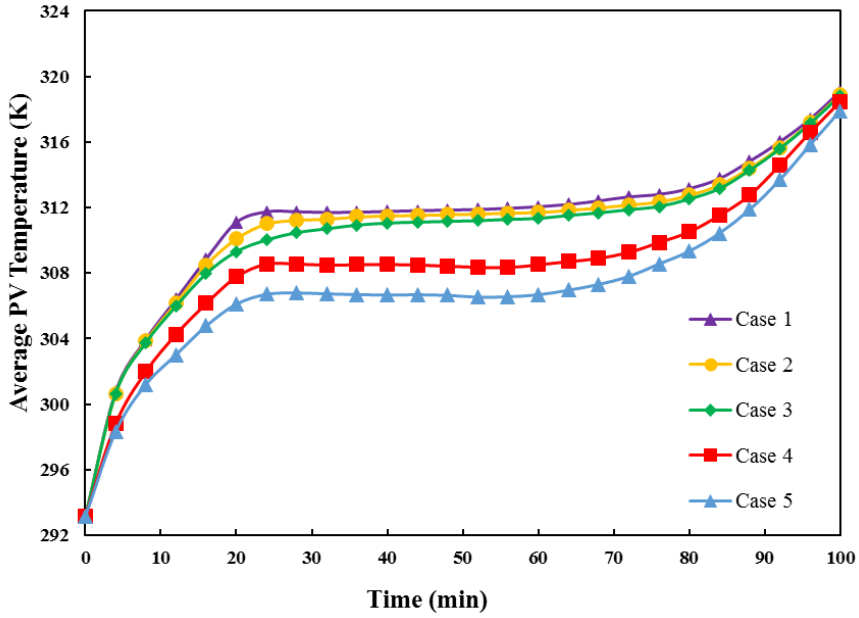

Fig. 13. Mean temperature of the photovoltaic module during a simulation of 100 minutes for a variety of fin shapes

Figure 14 demonstrates that the highest electrical efficiency is achieved in the case of dual-branch and triple-branch fins. On the other hand, the application of needle-shaped fins results in lower cooling performance compared to the conventional rectangular fins (Fig. 13). Thus, the PV-PCM system with needle-shaped fins has significantly lower electrical efficiency compared to the PVPCM module system with rectangular ones.

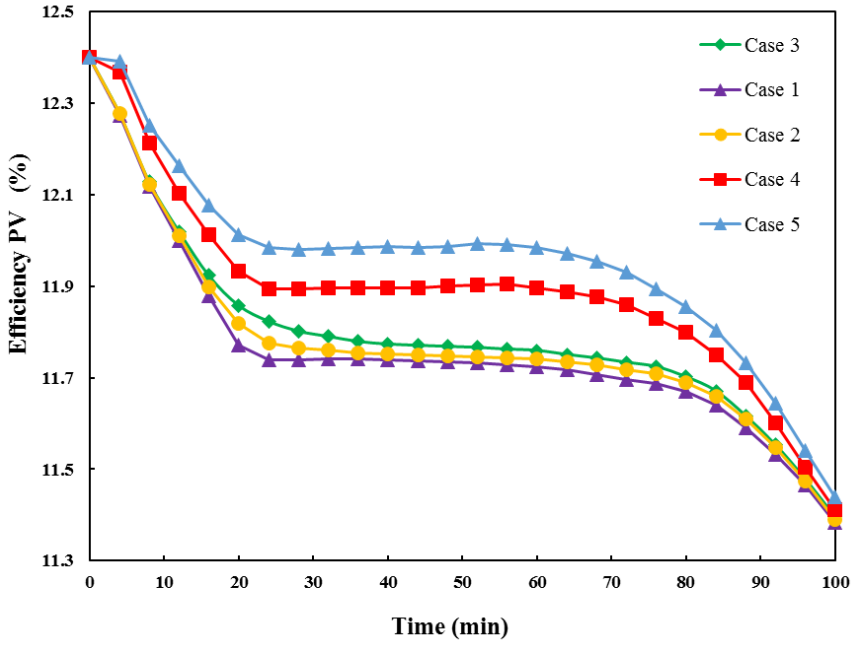

Fig. 14. Electrical efficiency of the photovoltaic module during a simulation of 100 minutes for a variety of fin shapes

4.4. Effect of fin type

The investigation on the effect of fin length represented that for the case with the longest fins, the best cooling performance of fins is achieved. Therefore, to obtain the optimum closed enclosure of fins, the effect of the application of different fin types on the thermal performance of fins has been investigated (Fig.15). In enclosed fin types, the significant improvement of conductive heat transfer compensates for the poor convection caused by disrupted natural convection of molten PCM. Figure15 illustrates the effect of employing different enclosed fin types on the liquid mass fraction of PCM at T=40mins. As seen, the maximum PV panel-PCM heat extraction is obtained for case 4 with triangle fins (Fig. 16).

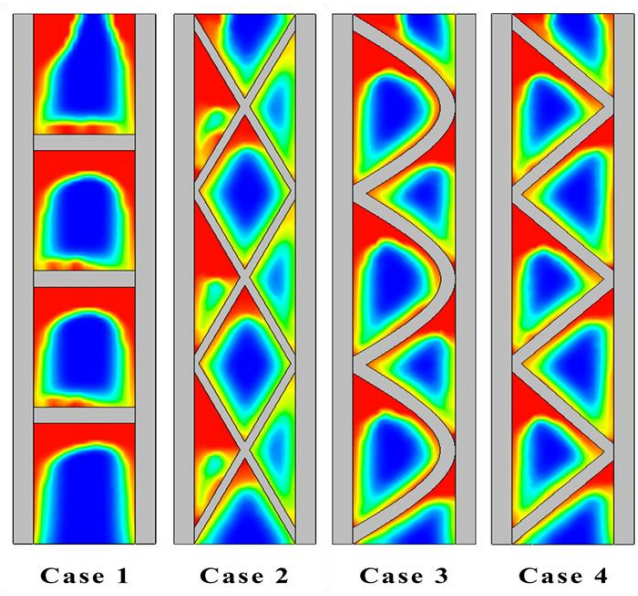

Fig. 15. Liquid mass fraction of phase change material at T=40mins, for different fin types

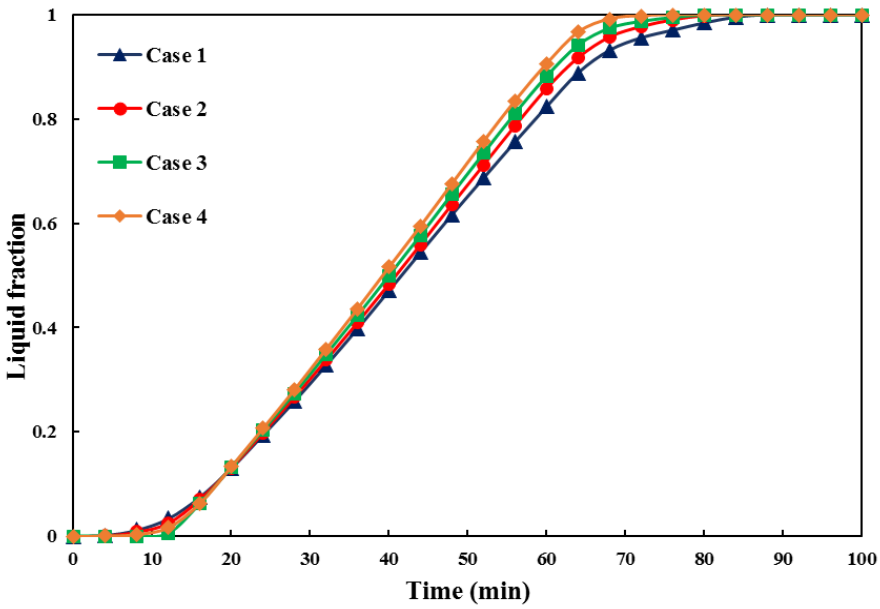

Fig. 16. Transient liquid mass fraction for different fin types

Figures 17 and 18 represent the effect of various enclosed fins on the average electrical efficiency and operating temperature of PV. The results indicate 0.48% and 0.57% average augmentation in the operating temperature and electrical performance of PV system for the case of triangle fin type is obtained, compared to case 1, with rectangular enclosed fins.

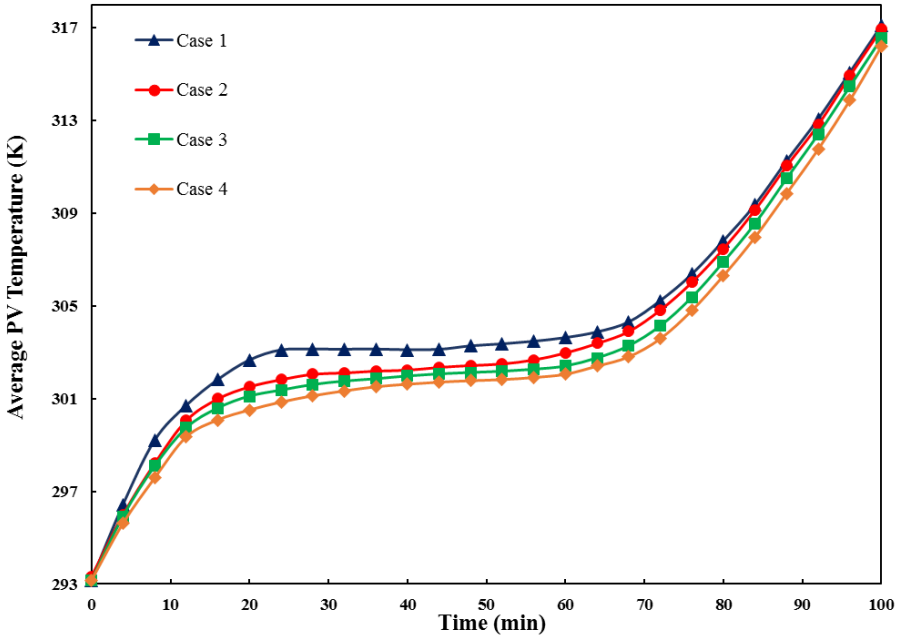

Fig. 17. The mean PV temperature during 100 minutes of simulation for different fin types

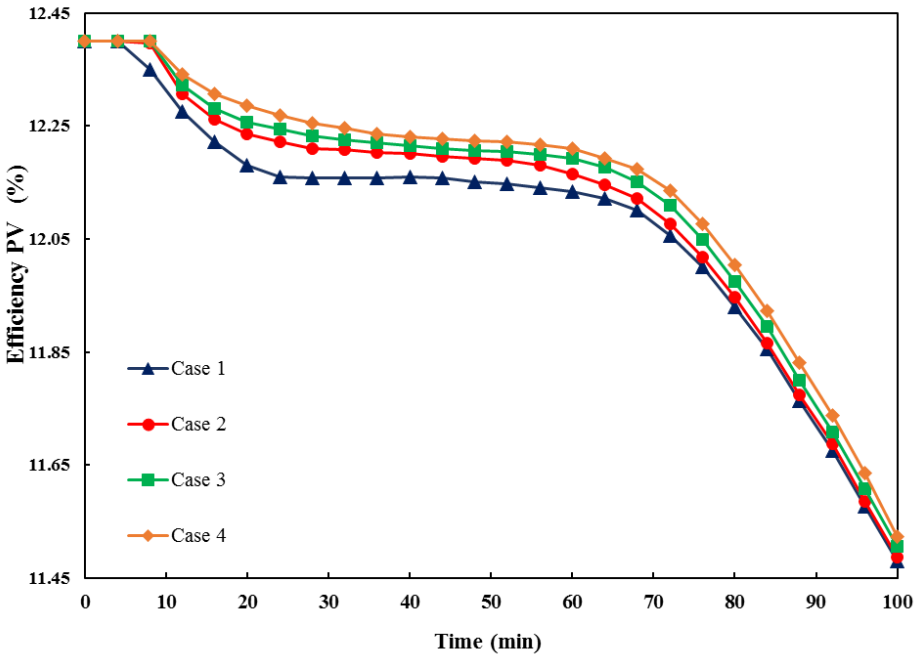

Fig. 18. Electrical efficiency of the photovoltaic module during a simulation of 100 minutes for a variety of fin types

4.5. Effect of employed fin material

The effects of fin materials on the phase alteration procedure of PCM as well as the overall performance of fins were studied through a comprehensive assessment. Copper and aluminum are used as fin materials to study the effect of fin material on the thermal conductivity of PCM. Figure 21 represents the liquid fraction of phase change material for the cases with no fin, two fins, and four fins. The results demonstrate that due to the higher thermal conductivity of copper, by employing copper fins compared to aluminum ones, lower operating temperature and subsequently higher efficiency is achieved (Figs. 19 & 20).

As mentioned before, PCM can also perform as thermal heat energy storage. Thus, it is essential to investigate the impacts of fin materials on the PCM's energy storage capacity. The comparative results represent that in the case of copper fins, due to the higher value of ρC_p, higher heat storage is achieved.

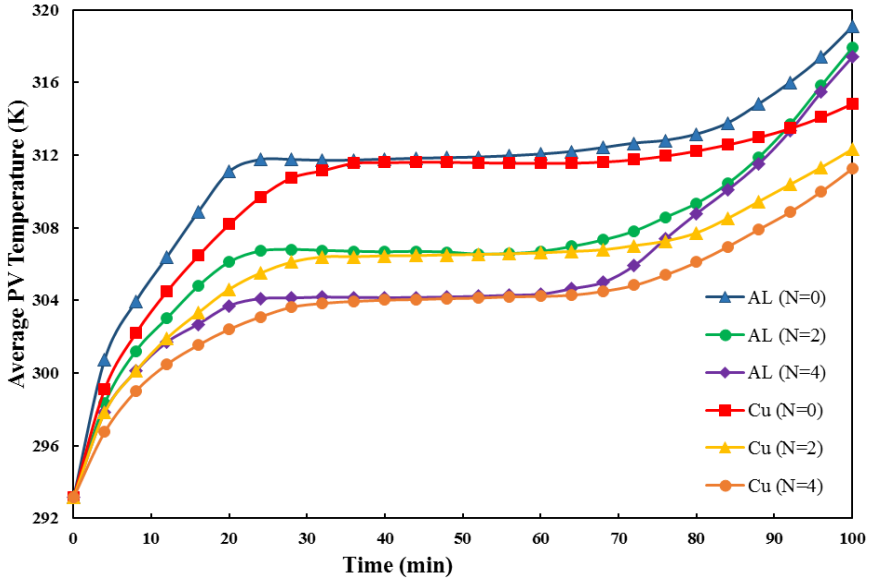

Fig. 19. Average temperature of PV panel for PV-PCMs with different fin materials and fin numbers

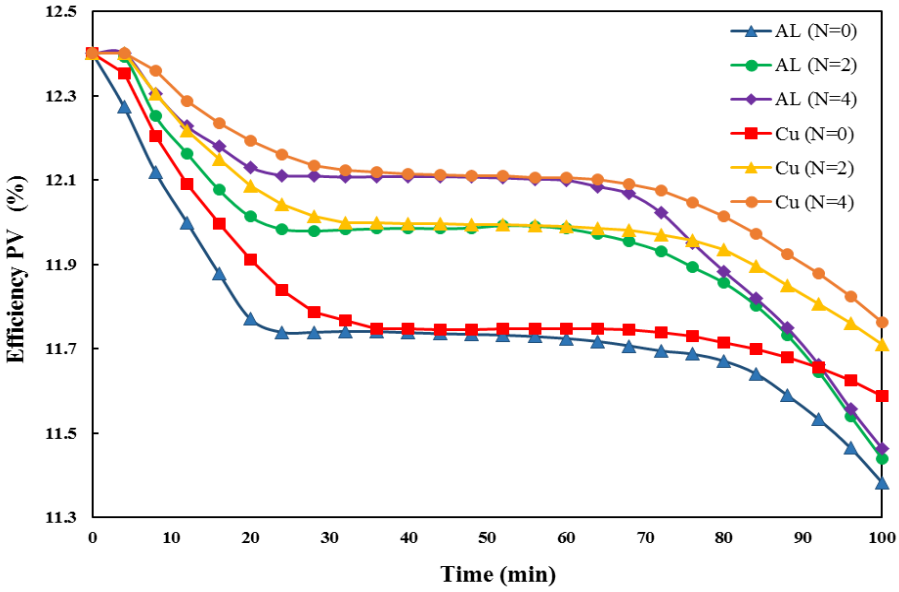

Fig. 20. Electrical efficiency of PV panel for PV-PCMs with different fin materials and fin numbers

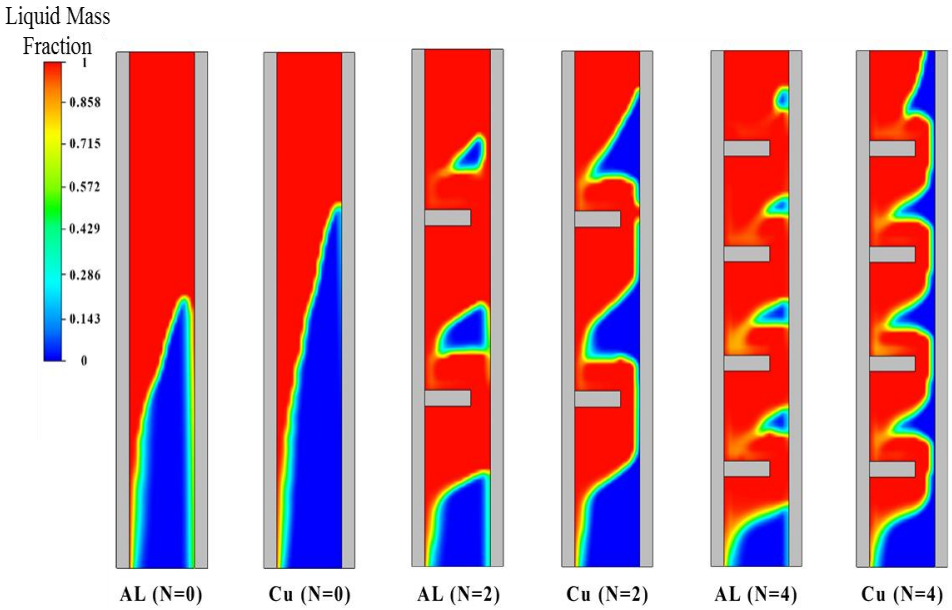

Fig. 21. Liquid mass fraction of PCM with different fin materials and fin numbers

4.6. Effect of PCM encapsulation type

The optimal design of PCM encapsulation was obtained by assessing the phase alteration procedure of PCM in PV-PCM systems with innovative non-rectangular designs (Fig. 22), which were compared to the rectangular design. The ratio of the top PCM container wall to the bottom wall for cases 1 to 5 are, $\frac{3}{1}$, $\frac{5}{3}$, 1, $\frac{3}{5}$, and $\frac{1}{3}$, respectively.

The liquid mass fraction of PCM during exposure to solar radiation for 100 min for non-rectangular and rectangular PCM encapsulations is illustrated in Fig. 23. Since the convective heat transfer is dominant at the initial phase change procedure, the movement of the phase change material's melt front is almost parallel to the right wall of the container for any definite type of encapsulation. In the case of employing non-rectangular encapsulations 1 and 2, the amount of PCM at the upper regions is higher. Due to the increase of available molten PCM for natural convection, the quasi-steady convective heat transfer and subsequently the phase change rate of PCM elevates (Fig. 23).

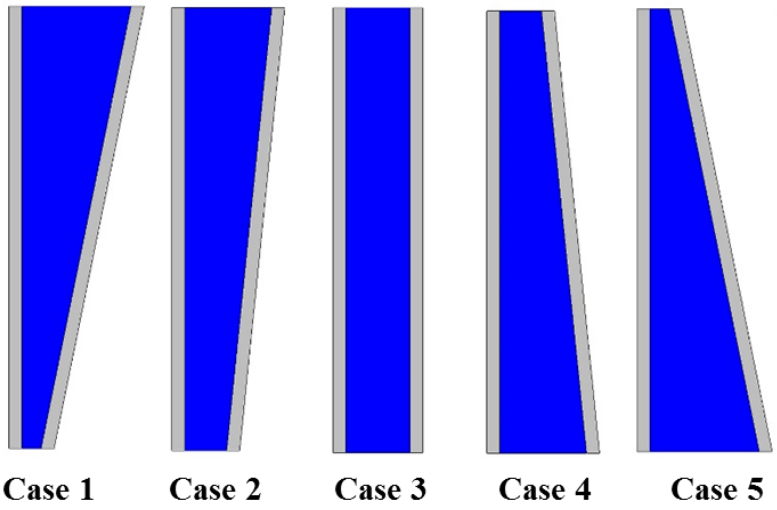

Fig. 22. Schematic of rectangular and non-rectangular PCM encapsulation designs

Although the encapsulation designs 1 and 2 impose desirable impacts on improving the PCM melting rate, the heat transfer by PCM was worsened and the phase alteration procedure was prolonged through encapsulation designs 4 and 5 in comparison to the rectangular designs 3. Figures 24 and 25 display the impacts of PCM encapsulation kind on the efficiency and average temperature of the PVPCM module.

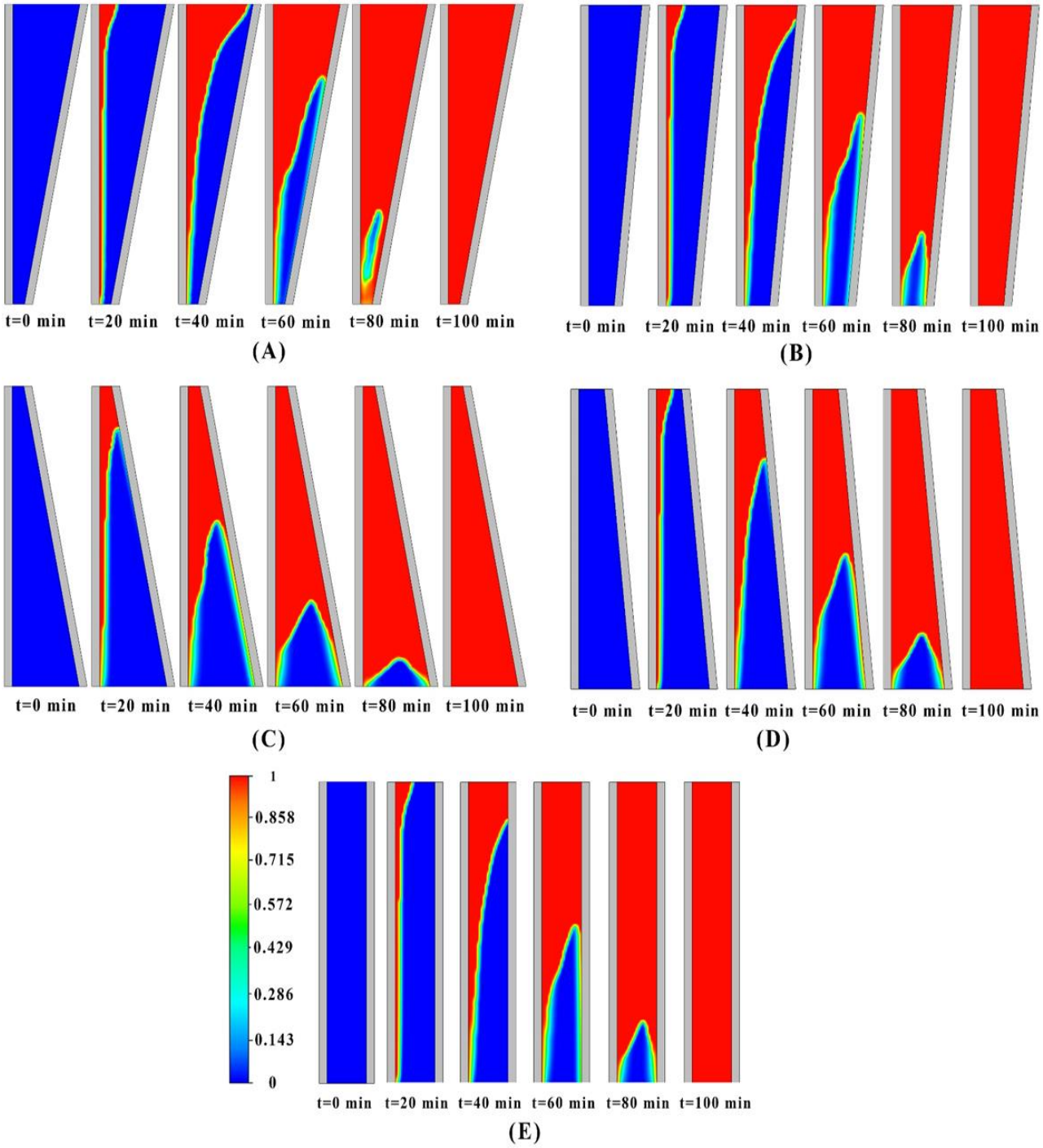

Fig. 23. Liquid mass fraction of PCM for a variety of PCM encapsulation types

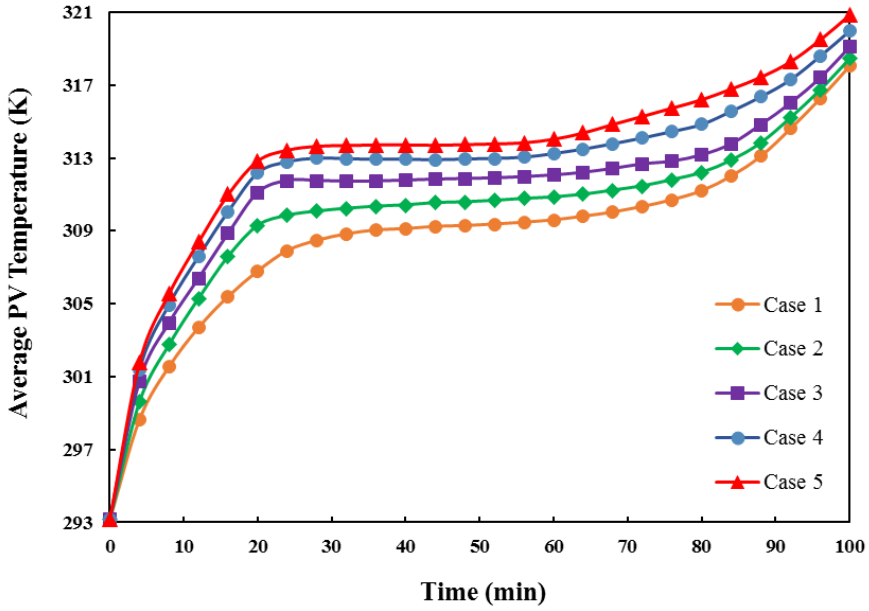

Fig. 24. Average temperature of the PV module for a variety of encapsulation designs during 100 minutes

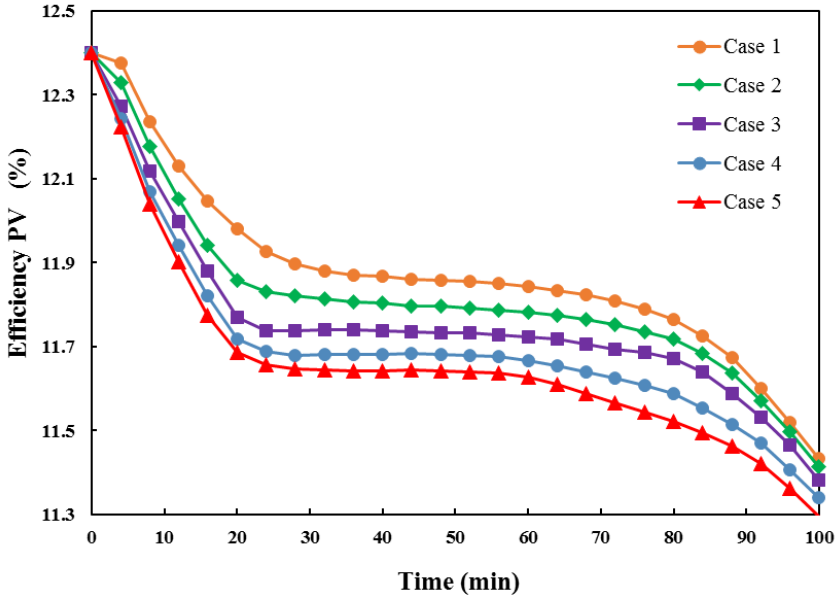

Fig. 25. Electrical efficiency of the PV module for a variety of encapsulation designs during 100 minutes

4.7. Effect of the inclination angle of phase change material container

Since PCM has weak thermal conductivity, there is considerably slower heat transfer between solid and molten PCM. However, this procedure can be accelerated by the natural convection of molten PCM. Figure 26 displays the PCM molten fraction for various inclination angles after 60 min. According to the comparison, the phase change process is significantly affected by the natural convection for higher angles (θ>30°). This can be clarified by increasing the gravity impact. Moreover, natural convection imposes a significantly effect on the lower angles. By increasing the PCM temperature, its density decreases. As a result, the liquid phase change material features lower density and moves upward, which is replaced by the phase change material featuring higher density. In addition, the natural movements of the convection vortices are restricted by lower inclination angles.

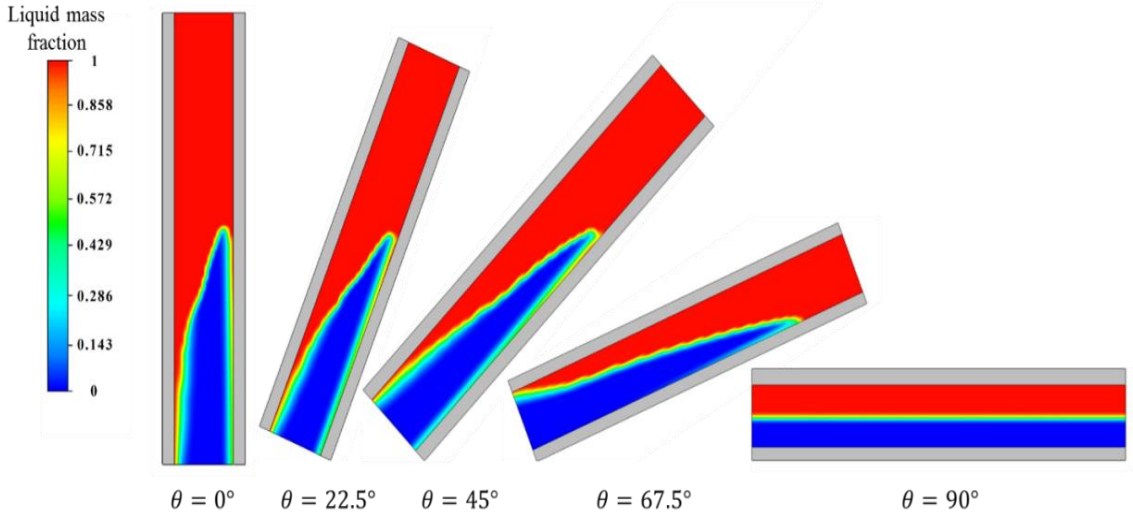

Fig. 26. Liquid mass fraction of phase change material at t=60min for a variety of inclination angles of the PVPCM module

Figures 27 and 28 present the contribution of the system's inclination angle to the electrical efficiency and average temperature of photovoltaic panels in the course of a solar radiation period of 100 minutes. According to the results, the lower average working temperature of the PV panel is obtained by the increased inclination angle as a result of the improved heat transfer by PCM. According to the previous arguments, the average temperature severely affects the electrical performance of photovoltaic panels. As a result, as is evident in Fig. 28, larger inclination angles result in better electrical efficiency of photovoltaic systems, which is ascribable to the augmented natural convection.

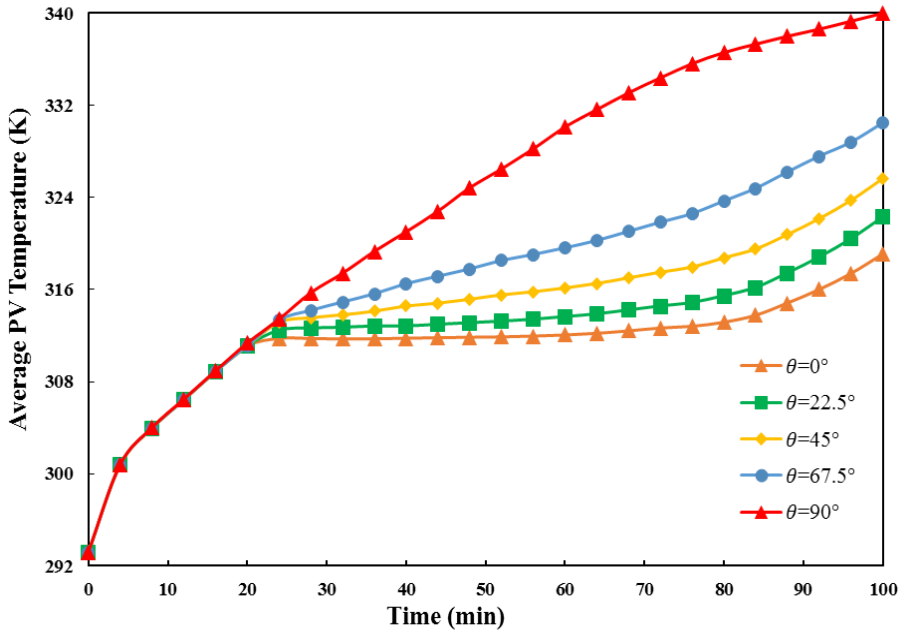

Fig. 27. Mean temperature of the photovoltaic module during 100 minutes of simulation for a variety of inclination angles

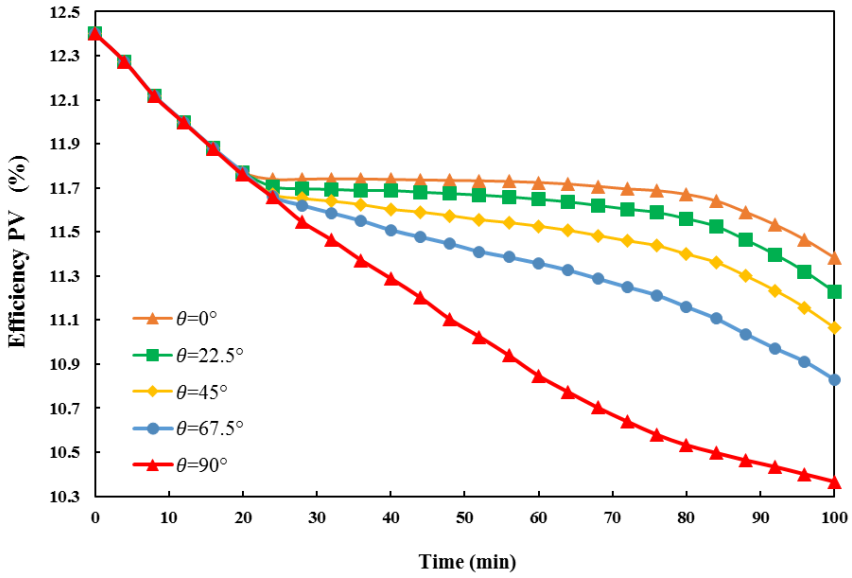

Fig. 28. Electrical efficiency of the photovoltaic module during 100 minutes of simulation for a variety of inclination angles

5. Conclusions

Also, a 2D numerical simulation is conducted to examine the effect of geometrical specifications of fins on the electrical efficiency and cooling performance of a finned phase change material integrated PV system. The effect of geometrical characteristics of fins such as length, vertical position, shape and type of fins, and additionally the inclination angle and type of PCM encapsulation are considered. The results obtained in the present study are summarized as follows:

- Through the maximum-length fins (20 mm), the efficiency and average temperature of the PV panel are enhanced by 3.5% and 2.7%, respectively.
- The weak thermal conductivity of PCM restricts the heat transfer in the lower sections of the PCM domain. Therefore, the application of a single fin in the lower parts has proven to be more effective.
- According to the findings, the average temperature of PV is considerably reduced leading to the maximum efficiency by using triple branch-shaped fins.
- Via triangle type of fins, the electrical efficiency and temperature of PV panels are improved by 0.57% and 0.48% in comparison to enclosed conventional rectangular fins.
- Due to insignificant enhancement in the case of application of copper fins and higher cost of copper fins, compared to the aluminum fins, use of copper fins is not suggested.
- Results indicate that application of PCM enclosures with higher ratio of top to bottom wall length, results in higher melting rate of PCM and consequently better cooling performance of PCM.

References

[1] R. Kumar, V. Deshmukh, and R. Singh Bharj, "Performance enhancement of photovoltaic modules by nanofluid cooling: A comprehensive review," Energy Res., vol. 44, no. 8, pp. 6149–6169, 2020.

[2] K. A. Emery et al., "Temperature dependence of photovoltaic cells, modules and systems," Conf. Rec. IEEE Photovolt. Spec. Conf. 1996, pp. 1275–1278, 1996.

[3] Akshayveer, A. Kumar, A. P. Singh, and O. P. Singh, "Effect of novel PCM encapsulation designs on electrical and thermal performance of a hybrid photovoltaic solar panel," Sol. Energy, vol. 205, pp. 320–333, 2020.

[4] H. Ami Ahmadi, N. Variji, A. Kaabinejadian, M. Moghimi, and M. Siavashi, "Optimal design and sensitivity

analysis of energy storage for concentrated solar power plants using phase change material by gradient metal foams," J. Energy Storage, vol. 35, 2021, doi: https://doi.org/10.1016/j.est.2021.102233.

[5] A. Ghahremannezhad, H. Xu, M. R. Salimpour, P. Wang, and K. Vafai, "Thermal Performance Analysis of Phase Change Materials (PCMs) Embedded in Gradient Porous Metal Foams," Appl. Therm. Eng., vol. 179, p. 115731, 2020.

[6] N. Asfattahi et al., "Improved thermo-physical properties and energy efficiency of hybrid PCM/graphene-silver nanocomposite in a hybrid CPV/thermal solar system," J. Therm. Anal. Calorim., 2020.

[7] A. Ejaz, F. Jamil, and H. Muhammad Ali, "A novel thermal regulation of photovoltaic panels through phase change materials with metallic foam-based system and a concise comparison: An experimental study," Sustain. Energy Technol. Assess., vol. 49, p. 101726, 2022.

[8] A. Naghdbishi, M. Eftekhari Yazdi, G. Akbari, "Numerical study on the performance of a glazed photovoltaic thermal system integrated with phase change material (GPVT/PCM): on the contribution of PCM volumetric fraction and environmental temperature, " Energy Equipment and Systems, vol. 10, p. 137-168, 2022.

[9] S. Rahmanian, H. Rahmanian-Koushkaki, P. Omidvar, and A. Shahsavar, "Nanofluid-PCM heat sink for building integrated concentrated photovoltaic with thermal energy storage and recovery capability," Sustain. Energy Technol. Assess., vol. 46, p. 101223, 2021.

[10] H. E. Abdelrahman, M. H. Wahba, H. A. Refaey, M. Moawad, and N. S. Berbish, "Performance enhancement of photovoltaic cells by changing configuration and using PCM (RT35HC) with nanoparticles Al2O3," Sol. Energy, vol. 177, pp. 665–671, 2019.

[11] M. Shirinbakhsh, N. Mirkhani, B. Sajadi, "Optimization of the PCM-integrated solar domestic hot water system under different thermal stratification conditions," Energy Equipment and Systems, vol. 4, p. 271-279, 2016.

[12] M. Sheikholeslami, A. Ghasemi, Z. Li, A. Shafee, and S. Saleem, "Influence of CuO nanoparticles on heat transfer behavior of PCM in solidification process considering radiative source term," Int. J. Heat Mass Transf., vol. 126, pp. 1252–1264, 2018.

[13] P. H. Biwole, P. Eclache, and F. Kuznik, "Phase-change materials to improve solar panel's performance," Energy Build., vol. 62, pp. 59–67, 2013.

[14] B. Hadidi, F. Veysi, "Numerical investigation of the simultaneous utilization of multiple phase change materials in the performance of thermal management system combined with heat sink," Energy Equipment and Systems, vol. 11, p. 455-481, 2023.

[15] W.-B. Ye, "Enhanced latent heat thermal energy storage in the double tubes using fins," J. Therm. Anal. Calorim., vol. 128, no. 1, pp. 533–540, 2016.

[16] S. Rashidi, J. Abolfazli Esfahani, and N. Karimi, "Porous materials in building energy technologies—A review of the applications, modelling and experiments," Renew. Sustain. Energy Rev., vol. 91, pp. 229–247, 2018.

[17] J. M. Mahdi and E. C. Nsofor, "Multiple-segment metal foam application in the shell-and-tube PCM thermal energy storage system," J. Energy Storage, vol. 20, pp. 529–541, 2018.

[18] A. Hussain, C. Y. Tso, and C. Y.H.Chao, "Experimental investigation of a passive thermal management system for high-powered lithium ion batteries using nickel foam-paraffin composite," Energy, vol. 115, pp. 209–218, 2016.

[19] H. Badenhorst, "A review of the application of carbon materials in solar thermal energy storage," Sol. Energy, vol. 192, no. 1, pp. 35–68, 2019.

[20] A. I. A. Al-Musawi, A. Taheri, A. Farzanehnia, M. Sardarabadi, and M. Passandideh-Fard, "Numerical study of the effects of nanofluids and phase-change materials in photovoltaic thermal (PVT) systems," J. Therm. Anal. Calorim., vol. 137, pp. 623–636, 2019.

[21] P. M. Kumar, K. Mylsamy, K. Alagar, and K. Sudhakar, "Investigations on an evacuated tube solar water heater using

hybrid-nano based organic phase change material," Int. J. Green Energy, pp. 872–883, 2020.

[22] M. K. Pasupathi, K. Alagar, M. J. Stalin P., M. M. M., and G. Aritra, "Characterization of Hybrid-nano/Paraffin Organic Phase Change Material for Thermal Energy Storage Applications in Solar Thermal Systems," Energies, vol. 13, no. 19, 2020.

[23] S. Khanna, K. S. Reddy, and T. K. Mallick, "Optimization of finned solar photovoltaic phase change material (finned pv pcm) system," Int. J. Therm. Sci., vol. 130, pp. 313–322, 2018.

[24] M. L. Benlekkam, D. Nehari, and H. I. Madani, "The thermal impact of the fin tilt angle and its orientation on performance of PV cell using PCM," Int. J. Heat Technol., vol. 36, pp. 919–926, 2018.

[25] S. Khanna, K. S. Reddy, and T. K. Mallick, "Effect of climate on electrical performance of finned phase change material integrated solar photovoltaic," Sol. Energy, vol. 174, pp. 593–605, 2018.

[26] S. Khanna, K. S. Reddy, and T. K. Mallick, "Performance analysis of tilted photovoltaic system integrated with phase change material under varying operating conditions," Energy, vol. 133, p. 887–899, 2017.

[27] A. Ahmad, H. Navarro, S. Ghosh, Y. Ding, and J. N. Roy, "Evaluation of New PCM/PV Configurations for Electrical Energy Efficiency Improvement through Thermal Management of PV Systems," Energies, vol. 14, p. 4130, 2021.

[28] Z. Rostami, N. Heidari, M. Rahimi, and N. Azimi, "Enhancing the thermal performance of a photovoltaic panel using nano-graphite/paraffin composite as phase change material," J. Therm. Anal. Calorim., 2021.

[29] A. Naseer et al., "Role of phase change materials thickness for photovoltaic thermal management," Sustain. Energy Technol. Assess., vol. 49, p. 101719, 2022.

[30] "Rubitherm GmbH, Rubitherm Data Sheet, Rubitherm GmbH, Hamburg." 2000.

[31] D. L. Evans and L. W. Florschuetz, "Cost studies on terrestrial photovoltaic power systems with sunlight concentration," Sol. Energy, vol. 19, no. 3, p. 255–262, 1977.